$(e, e'p)$ Reactions on ^{207}Pb and ^{209}Bi Through Isobaric Analog States and the Matrix Elements for the First-Forbidden β^- Decay

K. Shoda, A. Suzuki, M. Sugawara, T. Saito, H. Miyase, and S. Oikawa
Laboratory of Nuclear Science, Faculty of Science, Tohoku University, Tomizawa, Sendai, Japan
(Received 1 June 1970; revised manuscript received 23 November 1970)

The radiative widths of the $E1$ transition through the ground isobaric analog states of ^{207}Tl and ^{209}Pb in ^{207}Pb and ^{209}Bi, respectively, were determined from the cross section of the $(e,e'p)$ reaction. The results are 98 and 140 eV, respectively, after the correction for the interference from the continuous part of the reaction. They correspond to an effective charge of 0.56 and 21, respectively. The $E1$ matrix elements were determined and used for the estimation of β matrix elements $|i\xi\text{“}\int\vec{r}\text{”}|$. The result is 0.055 in natural units ($\hbar=c=m_e=1$) for the β-decay $^{207}\mathrm{Tl}(3s_{1/2}{}^{-1})\rightarrow{}^{207}\mathrm{Pb}(3p_{1/2}{}^{-1})$. In the case of $^{209}\mathrm{Pb}(2g_{9/2})\rightarrow{}^{209}\mathrm{Bi}(1h_{9/2})$, the result is 0.043, which is much larger than the theoretical estimate. For the $E1$ isobaric analog states of the first excited state of ^{209}Pb in ^{209}Bi, the radiative width and the effective charge were also determined to be 170 eV and 0.46, respectively.

I. INTRODUCTION

Measurements of the radiative strength of the $E1$ transition through isobaric analog states (hereafter referred to as IAS) should provide a powerful method to study the spectroscopy of the relevant states. The radiative width of a single level can be determined not only from the rate of the γ decay of the level but also from the cross section of the photoabsorption, which is an inverse process of γ decay. In the case of IAS, the photoabsorption cross section is almost equal to the (γ,p) cross section because the neutron emission from the IAS is forbidden by the isospin selection rule.

When the directions of the scattered electrons are not selected, the $(e,e'p)$ reactions are mainly dependent on the strong forward scattering of electrons. The momentum transfer in this case is equal to that of the photoreaction. Therefore the $(e,e'p)$ process is analogous to the (γ,p), and then the radiative width of the IAS can be obtained from the $(e,e'p)$ experiments, as well as the (γ,p) ones. From an experimental point of view, the former experiment seems more convenient for beam handling and for the determination of the dose of the incident beam, *etc.*

The nuclei ^{209}Bi and ^{207}Pb offer the two best cases for studying matrix elements because these nuclei can be well described as a single particle or a single hole added to the double-closed core ^{208}Pb. In the case of ^{209}Bi, the $E1$ radiative widths for the transitions from IAS of the ground state ($\frac{9}{2}^+$) and the first excited state ($\frac{11}{2}^+$) in ^{209}Pb to the ground state ($\frac{9}{2}^-$) are studied. All the related states are well described by single-particle states. In the case of ^{207}Pb, the radiative width from IAS of the ground state ($\frac{1}{2}^+$) in ^{207}Tl to the ground state ($\frac{1}{2}^-$) is studied. Well-established single-hole states are related in this transition. The level diagram and single-particle estimates of the states are shown in Fig. 1.

It will be interesting to estimate an effective charge of these transitions as a ratio of the experimental $E1$ matrix element to the theoretical single-particle one, because its deviation from unity reflects extra effects, for example, core polarization, etc.

The relation between the $E1$ matrix element and the first-forbidden β decay has been pointed out by several authors.[1-5] It has been difficult to extract the components of the β matrix element from experiments on the β decay. On the basis of the good quantum number of isospin, a β matrix element $\int\vec{r}$ can be estimated from the matrix element for the analogous $E1$ transition after correction for the lower-isospin contribution. Such an estimated matrix element $\int\vec{r}$ can be discussed in connection with an ft value of the β decay.

The β decays $^{207}\mathrm{Tl}\rightarrow{}^{207}\mathrm{Pb}$ and $^{209}\mathrm{Pb}\rightarrow{}^{209}\mathrm{Bi}$ have been theoretically studied by Damgaard and Winther.[6] These transitions are analogous to the above mentioned $E1$ transition, as shown in Fig. 1. Their theoretical matrix elements for $\int\vec{r}$ will be compared with the value estimated from the present experiment on the γ transition.

Ejiri *et al.*[3,4] estimated the $E1$ matrix element of IAS in ^{141}Pr with the $^{140}\mathrm{Ce}(p,\gamma_0)^{141}\mathrm{Pr}$ reaction to compare with the β-decay theory and obtained a reasonable result. In the present nuclei, the (p,γ_0) experiment cannot be realized on a ^{206}Tl target, which is unstable. The detection of γ rays from this reaction in this mass region should be difficult. In the present report, $E1$ matrix elements are determined with the $(e,e'p)$ reactions. The results will be compared with the theory of the single-particle shell model to determine the effective charge

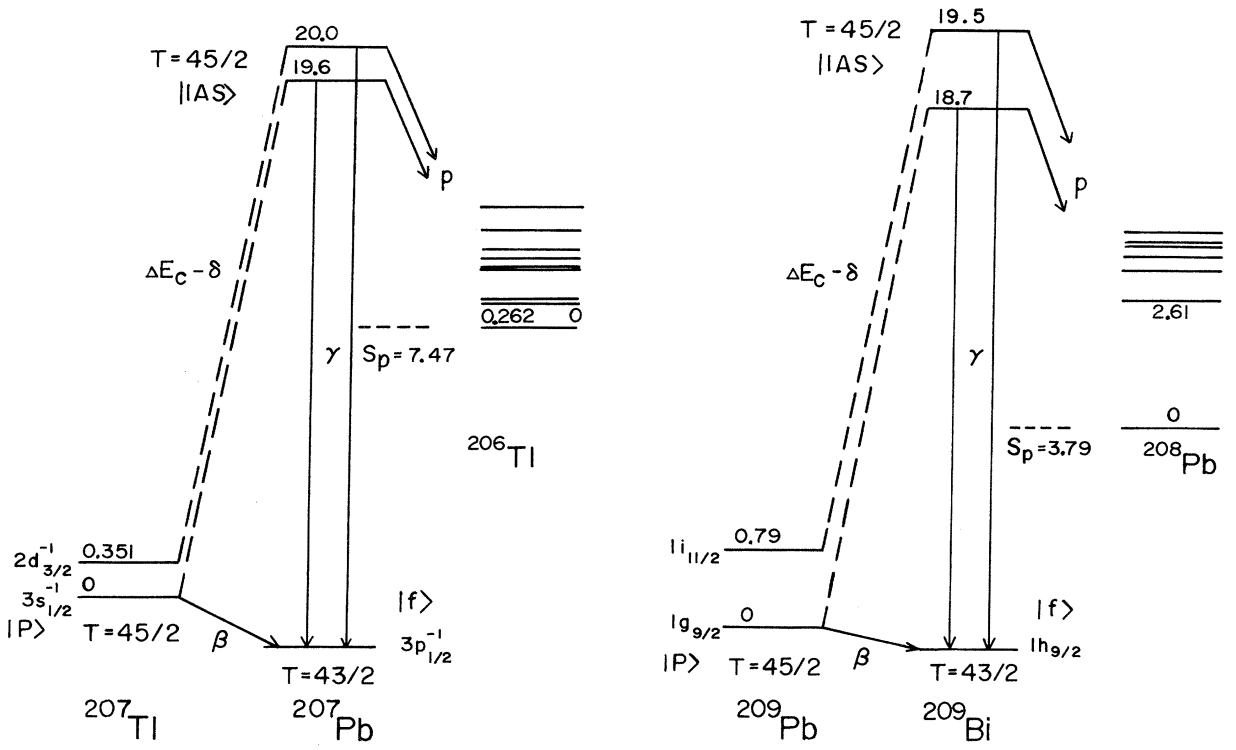

FIG. 1. The level diagram for the relations of $E1$ IAS and β decay. The energy levels are indicated in units of MeV. The single-particle configurations of the relevant states are indicated.

and to compare the β matrix element $\int \vec{r}$.

II. RELATED THEORY

A. $E1$ Transition Through IAS

The $E1$ radiative strength has usually been represented by the radiative width Γ_γ as follows:

$$\Gamma_\gamma = \hbar T^{E1}_{i\to f},$$
$$T^{E1}_{i\to f} = (16\pi/9)(1/\hbar)(\omega/c)^3 e^2 |M^\gamma|^2, \quad (1)$$
$$|M^\gamma|^2 = \sum_{\mu m_f} |M^\gamma_{1\mu}|^2 = \sum_{\mu m_f} |\langle f|\mathfrak{M}_{1\mu}|i\rangle|^2.$$

The $E1$ interaction operator $\mathfrak{M}_{1\mu}$ can be well approximated by

$$\mathfrak{M}_{1\mu} = rY_{1\mu}. \quad (2)$$

When the related states are well described by a particle or a hole, the $E1$ matrix element can be calculated from the single-particle shell model.

$$M^\gamma_{1\mu} = \left\langle f \left| \sum_{\lambda\nu} \left[\left(1 - \frac{Z}{A}\right) \langle \nu | rY_{1\mu} | \lambda \rangle_p a_\nu^\dagger a_\lambda - \frac{Z}{A} \langle \nu | rY_{1\mu} | \lambda \rangle_n b_\nu^\dagger b_\lambda \right] \right| i \right\rangle, \quad (3)$$

where the indices p and n show that the matrix elements are taken for the single-particle wave function of proton and neutron, and $a_\nu^\dagger$ (a_ν) and $b_\nu^\dagger$ (b_ν) are creation (annihilation) operators for a proton and a neutron, respectively. The IAS can be expressed in terms of the parent state $|P\rangle$ as follows:

$$|\mathrm{IAS}\rangle = [2(T+1)]^{-1/2} T_- |P\rangle, = [2(T+1)]^{-1/2} (\textstyle\sum a_\delta^\dagger b_\delta) |P\rangle, \quad (4)$$

where T is the isospin of the ground state $|f\rangle$. For the core-plus-single-particle or single-hole nuclei, such as ^{209}Bi and ^{207}Pb, the related states can be described as

$$|f\rangle = a_f^\dagger|0\rangle, |P\rangle = b_i^\dagger|0\rangle \quad \text{for core-plus-single-proton nucleus}, \quad (5)$$

$$|f\rangle = b_f|0\rangle, |P\rangle = a_i|0\rangle \quad \text{for core-plus-single-neutron-hole nucleus}. \quad (6)$$

Based on the relations Eqs. (3)–(5), the $E1$ matrix element for the IAS of $|P\rangle$ in the core-plus-single-proton nucleus can be reduced to

$$M^{\gamma}_{1\mu}(\mathrm{IAS}) = [2(T+1)]^{-1/2}\left[\left(1-\frac{Z}{A}\right)\langle f|rY_{1\mu}|P\rangle_p + \frac{Z}{A}\langle f|rY_{1\mu}|P\rangle_n\right]$$
$$= [2(T+1)]^{-1/2}\langle f|rY_{1\mu}|f\rangle \quad (7)$$
$$= [2(T+1)]^{-1/2} M^{\gamma}_{1\mu}(\mathrm{sp}),$$

where $M^{\gamma}_{1\mu}(\mathrm{sp})$ is a shell-model estimate of the single-particle transition. In Eq. (7), both matrix elements for a proton and a neutron in the same state are taken to be equal under the isospin independence of the nuclear force. In the case of the core-plus-single-neutron-hole nucleus, an analogous calculation gives

$$M^{\gamma}_{1\mu}(\mathrm{IAS}) = [2(T+1)]^{-1/2}\langle P|rY_{1\mu}|f\rangle$$
$$= [2(T+1)]^{-1/2} M^{\gamma}_{1\mu}(\mathrm{sp}). \quad (8)$$

From these results, the matrix element and the radiative width in these nuclei can be described by

$$|M^{\gamma}_{\mathrm{IAS}}| = [2(T+1)]^{-1/2}|M^{\gamma}_{\mathrm{sp}}|,$$
$$\Gamma^{\mathrm{IAS}}_{\gamma} = 2(T+1)^{-1}\Gamma_{\mathrm{sp}}. \quad (9)$$

If additional effects exist for the single-particle transition, they are reflected by an "effective charge" which is defined by

$$e_{\mathrm{eff}} = [2(T+1)]^{1/2}|M^{\gamma}_{\mathrm{IAS}}|/|M^{\gamma}_{\mathrm{sp}}|$$
$$= [2(T+1)\Gamma^{\mathrm{IAS}}_{\gamma}/\Gamma_{\mathrm{sp}}]^{1/2}. \quad (10)$$

B. Matrix Element of the First-Forbidden β Decay

The matrix element for β decay is related to the ft value. The relation for the present nuclei is given by the ξ approximation,

$$ft = 6250/[|M(0)|^2 + |M(1)|^2]$$
$$M(0) = \lambda_2 \text{“}\int \gamma_5\text{”} - i\xi\lambda \text{“}\int \vec{\sigma}\times\vec{r}\text{”}, \quad (11)$$
$$M(1) = \text{“}\int \vec{\alpha}\text{”} - i\xi \text{“}\int \vec{r}\text{”} + \lambda\xi \text{“}\int \vec{\sigma}\times\vec{r}\text{”}.$$

Damgaard and Winther[6] calculated the matrix elements using a well-defined single-particle wave function with a correction for the radial dependence of the electron wave function. If the experimental value of "$\int\vec{r}$" is obtained, the "effective β charge for g_V" is defined as $a = \text{“}\int\vec{r}\text{”}/(\text{“}\int\vec{r}\text{”})_{\mathrm{sp}}$ similarly to the $E1$-transition case.

Separate determination of "$\int\vec{r}$" from the β-decay experiment is difficult. Fujita[1,2] suggested a possibility for determining $\int\vec{r}$ from the $E1$ matrix element through the IAS. In this case, $\int\vec{r}$ does not include the correction for the electron wave function. Based on his discussion, the relation is introduced as follows:

$$\left|\int\vec{r}\right|^2 = \sum_{m_f}|\langle f|[\vec{r}_{\gamma}, T_-]|P\rangle|^2 .$$
$$= \frac{4\pi}{3}\sum_{\mu,m_f}|\langle f|[rY_{1\mu}, T_-]|P\rangle|^2 . \quad (12)$$

The state $|f\rangle$ is an eigenstate of T; therefore $T_+|f\rangle \approx 0$. By using this approximation and Eq. (4), the following relation is obtained

$$\langle f|[rY_{1\mu}, T_-]|P\rangle = \langle f|rY_{1\mu}T_-|P\rangle + \langle f|T_+rY_{1\mu}|P\rangle$$
$$= [2(T+1)]^{1/2}\langle f|rY_{1\mu}|\mathrm{IAS}\rangle . \quad (13)$$

Therefore, the relation is expressed by

$$\left|\int\vec{r}\right| = [2(T+1)(4\pi/3)]^{1/2}|M^{\gamma}_{\mathrm{IAS}}| . \quad (14)$$

III. EXPERIMENTAL ARRANGEMENT AND RESULTS

Self-supporting metal foils of ^{207}Pb (92.4% enriched, 5.9-mg/cm^2 thick) and ^{209}Bi (100% natural abundance, 6.9-mg/cm^2 thick) were bombarded by the electron beam from the Tohoku University linear accelerator. The energy distributions of protons from the $(e,e'p)$ reaction were measured for each run with a broad-range magnetic spectrometer at $\theta = 125.3°$. Examples of the results are shown in Fig. 2. The position expected for p_0 with the maximum end-point energy and that of p_0 through the ground IAS are shown by the dashed and solid vertical arrows, respectively. The main proton yields seem to correspond to those leaving the residual nuclei in excited states, especially in the case of the target nucleus ^{209}Bi.

The yields were determined from the total number of protons of $E_p \geq 7.4$ MeV for both nuclei. The contribution of the lower-energy protons was probably smaller than 15% and it was neglected in the present result. The number of bombarding electrons was measured with a secondary-emission monitor and a core monitor. The electron energy was changed by 100- or 200-keV steps. The resulting $(e,e'p)$ differential cross sections at $\theta = 125.3°$ are shown in Fig. 3. The theoretical positions of IAS are indicated in the figure accompanied with the single-particle configuration. They are in good agreement with the experimental result.

Neglecting small cross sections for large momentum transfer in the reaction, the cross section of the $(e,e'p)$ reaction can be expressed in the virtual-photon theory[7,8] as

$$\sigma_{(e,e'p)}(E_e) = C\int_0^{E_e}\sigma_{(\gamma,p)}(E)N(E,E_e)dE , \quad (15)$$

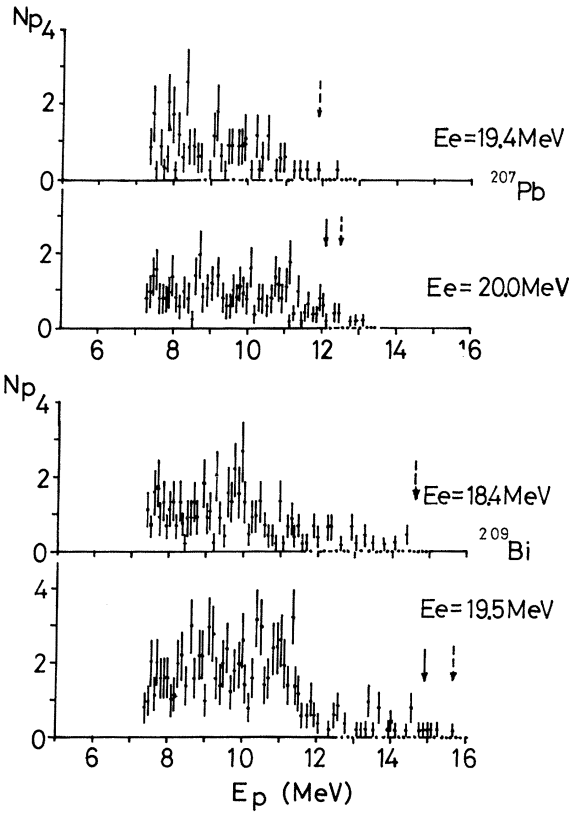

FIG. 2. Examples of the proton energy distributions. The positions expected for the maximum end-point energy of the protons are shown by the dashed vertical arrows. The solid vertical arrows indicate the position of p_0 through the ground IAS.

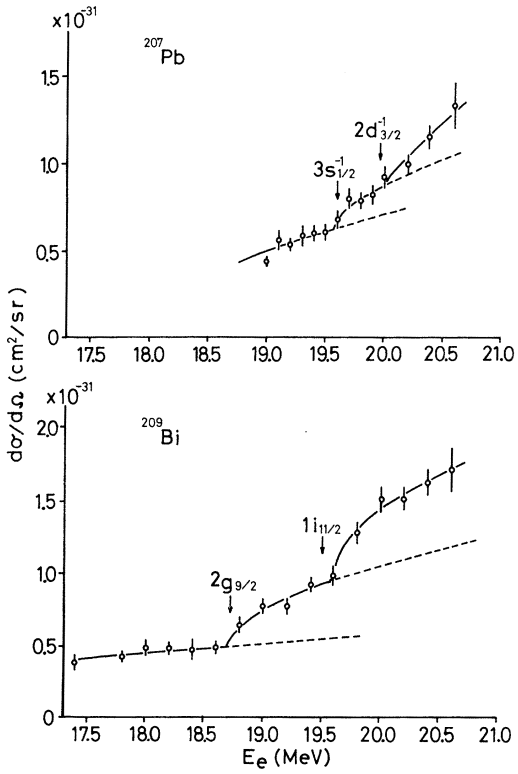

FIG. 3. Cross sections of the ^{207}Pb$(e,e'p)$ and ^{209}Bi$(e,e'p)$ reactions at $\theta=125.3°$. The positions of the IAS are shown by arrows.

where $\sigma_{(\gamma,p)}(E)$ is the photoproton cross section, $N(E,E_e)$ is a virtual-photon spectrum associated with an electron of energy E_e, and C is a constant depending on the experimental conditions. The virtual-photon spectra are continuous up to the energy E_e, similarly to those of the bremsstrahlung. Therefore, the cross section of the $(e,e'p)$ reaction is analogous to the photoproton yield curve obtained with bremsstrahlung. If $\sigma_{(\gamma,p)}$ includes a sharp resonance $\sigma^R_{(\gamma,p)}$ at E_x rising above a continuous cross section, the incremental cross section $\Delta\sigma_{(e,e'p)}(E_e)$ appears as follows:

$$\Delta\sigma_{(e,e'p)}(E_e)=CN(E_x,E_e)\int\sigma^R_{(\gamma,p)}\,dE\ . \tag{16}$$

This equation indicates that $\Delta\sigma_{(e,e'p)}(E_e)$ shows a shape proportional to $N(E_x,E_e)$. This causes a sudden increase in $\sigma_{(e,e'p)}(E_e)$ at E_x. In the present mass region, the resonance width of IAS is ordinarily about 250 keV,[9] which is small enough for the application of Eq. (16). Then the integrated cross section of the resonance $\int\sigma^R_{(\gamma,p)}dE$ can be obtained by

$$\int\sigma^R_{(\gamma,p)}\,dE=\frac{1}{C}\frac{\Delta\sigma_{(e,e'p)}(E_e)}{N(E_x,E_e)}. \tag{17}$$

The analysis can be applied to the differential cross section as shown in Fig. 3. Continuous parts of the cross sections were determined by extrapolating the lower-energy side as shown by the broken lines in the figure. The increment $\Delta(d\sigma_{(e,e'p)}/d\Omega)$ was obtained by subtracting this continuous part from the cross section. Using a relation similar to Eq. (17), the integrated cross section $\int[d\sigma^R_{(\gamma,p)}/d\Omega]dE$ was calculated. The constant C was determined by both geometrical calculation and normalization to the $^2_1$H$(e,e'p)$ and ^{12}C$(e,e'p)$ experiments. For $N(E_x,E_e)$, the equation for the $E1$ interaction for point charges was applied.[8]

The angular distribution should be well described by $I(\theta)=A+BP_2(\cos\theta)$ for the protons emitted through $E1$ IAS. Based on this angular distribution, $I(125.3°)=A$ holds, and the total number of protons integrated over all angles can be described by

$$\int I(\theta)d\Omega=4\pi A$$
$$=4\pi I(125.3°)\ . \tag{18}$$

Using this relation, the integrated cross section $\int\sigma^{R}_{(\gamma,p)}dE$ was calculated from the present differential cross section as follows:

$$\int \sigma^{R}_{(\gamma,p)}\,dE = 4\pi\int\left[\frac{d\sigma^{R}_{(\gamma,p)}}{d\Omega}\right]_{125.3^\circ} dE\ . \tag{19}$$

The integrated $E1$ resonant-absorption cross section $\int\sigma^{R}_{a}dE$ is related to the radiative width of the resonance Γ^{R}_{γ} by[10]

$$\int \sigma^{R}_{a}\,dE = (\pi\lambda\!\!\!^{-})^2\,\frac{2J_R+1}{2J_f+1}\,\Gamma^{R}_{\gamma}\ . \tag{20}$$

Neutron emission through $E1$ IAS is forbidden by the isospin selection rule; therefore, the related photodisintegration is mainly the (γ,p) reaction. We assumed $\sigma^{R}_{a}=\sigma^{R}_{(\gamma,p)}$ and determined Γ^{R}_{γ} by using Eq. (20). The result is shown in Table I.

An effect from interference between the IAS resonance and the giant-dipole resonance is discussed in the Appendix. Based on this result, the ratio of the integrated noninterferent cross section for the IAS $\int\sigma^{IAS}_{(\gamma,p)}dE$ to that of the interferent-resonance $\int\sigma^{R}_{(\gamma,p)}dE$ is given by

$$R=\frac{\int\sigma^{IAS}_{(\gamma,p)}dE}{\int\sigma^{R}_{(\gamma,p)}dE}=1+2\eta\left[1\pm\left(1+\frac{1}{\eta}\right)^{1/2}\right],$$

$$\eta=\zeta\cos^2(\phi_D-\phi_{IAS})\,\frac{\frac{1}{2}\pi\Gamma^{IAS}_{t}\sigma^{GD}_{(\gamma,p)}(E_{IAS})}{\int\sigma^{R}(\gamma,p)dE}\ , \tag{21}$$

$$\zeta=\sigma^{D}_{J(\gamma,p)}\ (E_{IAS})/\sigma^{GD}_{(\gamma,p)}(E_{IAS})\ .$$

From the relation (20), this ratio is also equal to the ratio between the noninterferent radiative width Γ^{IAS}_{γ} and Γ^{R}_{γ}; i.e. $R=\Gamma^{IAS}_{\gamma}/\Gamma^{R}_{\gamma}$. The width Γ^{IAS}_{γ} was estimated from this ratio. In the actual calculation, the phase difference $\phi_D-\phi_{IAS}$ is approximated as zero. As discussed in Ref. 4, this approximation should be reasonable. The total width of the IAS, Γ^{IAS}_{t}, is chosen as 250 KeV.[9] The $\sigma^{GD}_{(\gamma,p)}(E_x)$ was estimated from the increment of the continuous part of the $(e,e'p)$ cross section in the vicinity of the IAS using approximately the photon difference method. The factor ζ was roughly assumed to be

$$\zeta=(2J_R+1)\Big/\sum_{J_k=J_{f-1}}^{J_f+1}(2J_k+1)\ .$$

The result for Γ^{IAS}_{γ} is also shown in Table I. In the table, the errors include statistical uncertainties only, and some additional systematical errors should be included, mainly based on the uncertainty of the values of the parameters in Eq. (21) for Γ^{IAS}_{γ}. The systematic errors are difficult to estimate exactly, but may be less than 30% in usual cases. The table also shows the experimental single-particle radiative width estimated as $2(T+1)\Gamma^{IAS}_{\gamma}$ using Eq. (9). Then it shows the ratio to the Weisskopf unit and also to the single-particle radiative width, which was calculated with a wave function using a diffuse potential and including a spin-orbit interaction.[11]

IV. DISCUSSION

As shown in Table I, the experimental radiative width indicates some hindrance effects in the $E1$ transition of the non-spin-flip type; i.e., $3s_{1/2}{}^{-1}\rightarrow 3p_{1/2}{}^{-1}$ in ^{207}Pb and $1i_{11/2}\rightarrow 1h_{9/2}$ in ^{209}Bi. However, in the case of an $E1$ transition of the spin-flip type; i.e., $2g_{9/2}\rightarrow 1h_{9/2}$ in ^{209}Bi; a large enhancement is found. Usually the theoretical $E1$ transition probability can be represented by a multiplication of two factors, a radial part and a statistical factor S,[12] as follows:

$$T^{E1}_{i\rightarrow f}=\frac{4}{9}\,\frac{1}{\hbar}\left(\frac{\omega}{C}\right)^3 e^2\left(\int^{\infty}\Re_f r\,\Re_i r^2 dr\right)^2 S(j_i,L,j_f)\ . \tag{22}$$

The factor S is of the order unity in the non-spin-flip transition, but it is less than $\frac{1}{10}$ in the spin-flip case. As this factor reduces Γ_{sp} in the latter case, a large value of $2(T+1)\Gamma^{IAS}_{\gamma}/\Gamma_{sp}$ results in the present case. If the ratio is taken to the Weisskopf unit in which the spin dependence is ignored ($S=1$), the results are nearly equal for all the cases, as shown in Table I. From the above comparison, the $2g_{9/2}\rightarrow 1h_{9/2}$ transition includes either a surprisingly large enhancement of the single-particle transition or some different modes which appear to be spin independent.

TABLE I. Radiative widths of $E1$ IAS in ^{207}Pb and ^{209}Bi. The errors include statistical uncertainties only.

Nucleus	Ground state	IAS	E_x (MeV)	Γ^{R}_{γ} (eV)	Γ^{IAS}_{γ} (eV)	$2(T+1)\Gamma^{IAS}_{\gamma}$ (keV)	$2(T+1)\frac{\Gamma^{IAS}_{\gamma}}{\Gamma_W}$	$2(T+1)\frac{\Gamma^{IAS}_{\gamma}}{\Gamma_{sp}}$
^{207}Pb	$\frac{1}{2}^-(3p_{1/2}{}^{-1})$	$\frac{1}{2}^+(3s_{1/2}{}^{-1})$	19.6	160±50	98±30	4.4±1.3	0.25±0.08	0.32±0.09
^{209}Bi	$\frac{9}{2}^-(1h_{9/2})$	$\frac{9}{2}^+(2g_{9/2})$	18.7	180±20	140±20	6.3±0.8	0.40±0.05	430±55
^{209}Bi	$\frac{9}{2}^-(1h_{9/2})$	$\frac{11}{2}^+(1i_{11/2})$	19.5	220±30	170±20	7.6±1.0	0.43±0.06	0.21±0.03

TABLE II. Matrix elements and "effective charge" for the single-particle $E1$ transition.

Nucleus	States Ground	States IAS	Matrix element (F) $\lvert M^{\gamma}_{\mathrm{IAS}}\rvert$	Matrix element (F) $\lvert\int\vec{r}\rvert$	e_{eff}
^{207}Pb	$3p_{1/2}{}^{-1}$	$3s_{1/2}{}^{-1}$	0.11 ± 0.02	1.5 ± 0.2	0.56 ± 0.08
^{209}Bi	$1h_{9/2}$	$2g_{9/2}$	0.14 ± 0.02	2.0 ± 0.2	21 ± 1
^{209}Bi	$1h_{9/2}$	$1i_{11/2}$	0.15 ± 0.02	2.0 ± 0.2	0.46 ± 0.03

An exact $E1$ operator is expressed by:

$$e\mathfrak{M}_{1\mu}=erY_{1\mu}-\frac{i\mu_p e\hbar\omega}{4mc^2}\,\vec{\sigma}\times\vec{r}\cdot[\mathrm{grad}(rY_{1\mu})]. \quad (23)$$

The matrix element of the second term is about 10^{-1} of the first term for the present spin-flip transitions. Therefore it is difficult to explain the large enhancement by the higher-order term of the interaction.

The effective charge e_{eff} is estimated with Eq. (10) as one kind of spectroscopic factor in the $E1$ transitions. The result is shown in Table II accompanied with the $E1$ matrix element $|M^{\gamma}_{\mathrm{IAS}}|$. In the non-spin-flip transition case, e_{eff} is about $\frac{1}{2}$ which is reasonable to expect from core-polarization effects.

The present experimental matrix element $|M^{\gamma}_{\mathrm{IAS}}|$ was used to estimate the corresponding β matrix element $|\int\vec{r}|$ with Eq. (14). The results are also shown in Table II. Under the assumption that the effect of the radial dependence of the electron wave function is equal to the theoretical one demonstrated by Damgaard and Winther,[6] the experimental value of the exact matrix elements $|\text{“}\int\vec{r}\text{”}|$ can be estimated from $|\int\vec{r}|$ multiplied by their theoretical ratio $\text{“}\int\vec{r}\text{”}/\int\vec{r}$. The β matrix elements $|i\xi\text{“}\int\vec{r}\text{”}|$ are compared in Table III with their theoretical single-particle values calculated from the same wave function as for the Γ_{sp} in the present paper. Damgaard and Winther also determined the value $\text{“}\int\vec{r}\text{”}$ for the best fit to the experimental ft value using their theoretical matrix elements. They estimated two possible "effective β charges for g_V," $a=0.60$ or 0.30, defined as the ratio to their single-particle matrix element. The estimation of the "effective β charge" a can be made from the present experimental matrix element. The values obtained in the two different ways are compared in Table III. In the case of β decay of ^{207}Tl, the present value agrees well with one of their values ($a=0.60$). Based on their analysis, this value corresponds to the "effective β charge for g_A" $b=\text{“}\int\vec{\sigma}\times\vec{r}\text{”}/(\text{“}\int\vec{\sigma}\times\vec{r}\text{”})_{\mathrm{sp}}=0.57$.

In the case of β decay of ^{209}Pb, $\text{“}\int\vec{r}\text{”}$ cannot be discussed exactly in relation to the ft value, because the ft value is mainly determined from the matrix element of order zero, $|M(0)|$, even though the matrix element $|i\xi\text{“}\int\vec{r}\text{”}|$ is considerably enhanced, as in the present experimental result.

ACKNOWLEDGMENTS

The authors are very grateful to Professor Y. Kojima and his crew for the beam operation. They thank Professor J. I. Fujita and Dr. K. Takahashi for their useful discussions and suggestions.

APPENDIX

The effect of the interference between the resonance of the IAS and giant-dipole (GD) resonance was calculated in a way similar to the case of the (p,γ) reaction.[4,13] Neglecting a contribution from compound processes, $\sigma_{(\gamma,p)}$ can be approximated as

$$\begin{aligned}\sigma_{(\gamma,p)}&=K^2|A_J^{\mathrm{IAS}}+\sum_{J'}A_{J'}^{\mathrm{D}}|^2\\&=K^2[|A_J^{\mathrm{IAS}}|^2+\sum_{J'}|A_{J'}^{\mathrm{D}}|^2+2\,\mathrm{Re}(A_J^{\mathrm{IAS}}A_J^{\mathrm{D}*})],\end{aligned} \quad (A1)$$

where K is a kinematical constant. The noninterferent cross section of the IAS, $\sigma^{\mathrm{IAS}}_{(\gamma,p)}$; the cross section corresponding to the interference, $\sigma^{\mathrm{IF}}_{(\gamma,p)}$; and the photoproton giant-resonance cross section, $\sigma^{\mathrm{GD}}_{(\gamma,p)}$, are defined as follows:

$$\begin{aligned}\sigma^{\mathrm{R}}_{(\gamma,p)}&=\sigma^{\mathrm{IAS}}_{(\gamma,p)}+\sigma^{\mathrm{IF}}_{(\gamma,p)}\,,\\\sigma^{\mathrm{IAS}}_{(\gamma,p)}&=K^2|A_J^{\mathrm{IAS}}|^2\,,\\\sigma^{\mathrm{IF}}_{(\gamma,p)}&=2K^2\,\mathrm{Re}(A_J^{\mathrm{IAS}}A_J^{\mathrm{D}*})\,,\\\sigma^{\mathrm{GD}}_{(\gamma,p)}&=\sum_{J'}\sigma^{\mathrm{D}}_{J',(\gamma,p)}=K^2\sum_{J'}|A_{J'}^{\mathrm{D}}|^2\,,\end{aligned} \quad (A2)$$

TABLE III. Comparison of the matrix element $|i\xi\text{“}\int\vec{r}\text{”}|$ in natural units ($\hbar=c=m_e=1$) and the "effective β charge for g_V," a, for the first-forbidden β decay. The errors include statistical uncertainties only.

Decay scheme P	Decay scheme f	Present experiment $\lvert i\xi\text{“}\int\vec{r}\text{”}\rvert$	Present experiment a	Theory (Ref. 6) $\lvert i\xi\text{“}\int\vec{r}\text{”}\rvert$	Theory (Ref. 6) a
^{207}Tl$(3s_{1/2}{}^{-1})$	^{207}Pb$(3p_{1/2}{}^{-1})$	0.055 ± 0.007	0.56 ± 0.08	0.099	0.60 or 0.30
^{209}Pb$(2g_{9/2})$	^{209}Bi$(1h_{9/2})$	0.043 ± 0.004	21 ± 1	0.0020	

where $\sigma^{D}_{J'(\gamma,p)} = K^2 |A^{D}_{J'}|^2$. A resonance type can be applied for A^{IAS}_{J} and $A^{D}_{J'}$:

$$A^{IAS}_{J} = i \frac{(\Gamma^{IAS}_{p}\Gamma^{IAS}_{\gamma})^{1/2} e^{i\phi_{IAS}}}{(E - E_{IAS}) + \frac{1}{2} i \Gamma^{IAS}_{t}} ,$$
$$A^{D}_{J'} = i \frac{(\Gamma^{D}_{p}\Gamma^{D}_{\gamma})^{1/2} e^{i\phi_{D}}}{(E - E_{D}) + \frac{1}{2} i \Gamma^{D}_{t}} . \quad \text{(A3)}$$

From Eqs. (A2) and (A3), the following relation is obtained:

$$K(\Gamma^{IAS}_{p}\Gamma^{IAS}_{\gamma})^{1/2} = \tfrac{1}{2}\Gamma^{IAS}_{t}[\sigma^{IAS}_{(\gamma,p)}(E_{IAS})]^{1/2} . \quad \text{(A4)}$$

Using Eqs. (A2) and (A4), Eqs. (A3) are expressed in the vicinity of the IAS

$$KA^{IAS}_{J} = \frac{\sigma^{IAS}_{(\gamma,p)}}{[\sigma^{IAS}_{(\gamma,p)}(E_{IAS})]^{1/2}} \frac{2}{\Gamma^{IAS}_{t}} \times [(E - E_{IAS}) e^{i(\phi_{IAS} + \pi/2)} + \tfrac{1}{2}\Gamma^{IAS}_{t} e^{i\phi_{IAS}}] ,$$
$$KA^{D}_{J} = [\sigma^{D}_{J(\gamma,p)}(E_{IAS})]^{1/2} e^{i\phi_{D}} = [\zeta \sigma^{GD}_{(\gamma,p)}(E_{IAS})]^{1/2} e^{i\phi_{D}} , \quad \text{(A5)}$$
$$\zeta = \sigma^{D}_{J(\gamma,p)}(E_{IAS}) / \sigma^{GD}_{(\gamma,p)}(E_{IAS}) ,$$

where $\Gamma^{IAS}_{t} \ll \Gamma^{D}_{t}$ is assumed. The interferent part $\sigma^{IF}_{(\gamma,p)}$ can be described from Eq. (A2) by using Eqs. (A5).

$$\sigma^{IF}_{(\gamma,p)} = \sigma^{IAS}_{(\gamma,p)} \left[\zeta \frac{\sigma^{GD}_{(\gamma,p)}(E_{IAS})}{\sigma^{IAS}_{(\gamma,p)}(E_{IAS})} \right]^{1/2} \frac{4}{\Gamma^{IAS}_{t}} \mathrm{Re}[(E - E_{IAS}) e^{i(\phi_{IAS} - \phi_{D} + \pi/2)} + \tfrac{1}{2}\Gamma^{IAS}_{t} e^{i(\phi_{IAS} - \phi_{D})}]$$
$$= \sigma^{IAS}_{(\gamma,p)} \left[\zeta \frac{\sigma^{GD}_{(\gamma,p)}(E_{IAS})}{\sigma^{IAS}_{(\gamma,p)}(E_{IAS})} \right]^{1/2} \frac{4}{\Gamma^{IAS}_{t}} [(E - E_{IAS}) \sin(\phi_{D} - \phi_{IAS}) + \tfrac{1}{2}\Gamma^{IAS}_{t} \cos(\phi_{D} - \phi_{IAS})] . \quad \text{(A6)}$$

Integrations are performed by considering that $\sigma^{IAS}_{(\gamma,p)}$ is an even function and the first term in Eq. (A6) is an odd function of $(E - E_{IAS})$. The results are

$$\int \sigma^{IAS}_{(\gamma,p)} dE = \tfrac{1}{2}\pi \Gamma^{IAS}_{t} \sigma^{IAS}_{(\gamma,p)}(E_{IAS}) , \quad \text{(A7)}$$

$$\int \sigma^{R}_{(\gamma,p)} dE = \int \sigma^{IAS}_{(\gamma,p)} dE + \int \sigma^{IF}_{(\gamma,p)} dE$$
$$= \left\{ 1 + 2 \left[\zeta \frac{\sigma^{GD}_{(\gamma,p)}(E_{IAS})}{\sigma^{IAS}_{(\gamma,p)}(E_{IAS})} \right]^{1/2} \cos(\phi_{D} - \phi_{IAS}) \right\} \int \sigma^{IAS}_{(\gamma,p)} dE$$
$$= \left\{ 1 + 2 \left[\zeta \frac{\sigma^{GD}_{(\gamma,p)}(E_{IAS})}{(2/\pi\Gamma^{IAS}_{t}) \int \sigma^{IAS}_{(\gamma,p)} dE} \right]^{1/2} \cos(\phi_{D} - \phi_{IAS}) \right\} \int \sigma^{IAS}_{(\gamma,p)} dE . \quad \text{(A8)}$$

Equation (A8) can be solved for $\int \sigma^{IAS}_{(\gamma,p)} dE / \int \sigma^{R}_{(\gamma,p)} dE = R$, and the following result is obtained:

$$R = \frac{\int \sigma^{IAS}_{(\gamma,p)} dE}{\int \sigma^{R}_{(\gamma,p)} dE} = 1 + 2\eta \left[1 \pm \left(1 + \frac{1}{\eta} \right)^{1/2} \right] \quad \eta = \zeta \cos^2(\phi_{D} - \phi_{IAS}) \frac{\tfrac{1}{2}\pi \Gamma^{IAS}_{t} \sigma^{GD}_{(\gamma,p)}(E_{IAS})}{\int \sigma^{R}_{(\gamma,p)} dE} . \quad \text{(A9)}$$

[1] J. I. Fujita, Phys. Letters 24B, 123 (1967).

[2] J. I. Fujita, Brookhaven National Laboratory Report No. BNL-837C-39, 1963 (unpublished), p. 340.

[3] H. Ejiri, P. Richard, S. Ferguson, R. Heffner, and D. Perry, Phys. Rev. Letters 21, 373 (1968).

[4] H. Ejiri, P. Richard, S. Ferguson, R. Heffner, and D. Perry, Nucl. Phys. A128, 388 (1969).

[5] A. Bohr and B. R. Mottelson, *Nuclear Structure* (W. A. Benjamin, Inc., New York, 1969), Vol. 1, p. 350, 408.

[6] J. Damgaard and A. Winther, Nucl. Phys. 54, 615 (1964).

[7] R. H. Dalitz and D. R. Yennie, Phys. Rev. 105, 1598 (1957).

[8] W. C. Barber and T. Wiedling, Nucl. Phys. 18, 575 (1960).

[9] W. R. Wharton, P. von Brentano, W. K. Dawson, and P. Richard, Phys. Rev. 176, 1424 (1968).

[10] E. Hayward, in *Nuclear Structure and Electromagnetic Interactions*, edited by N. MacDonald (Oliver and Boyd Publishers, London, England 1964), p. 141.

[11] J. Blomqvist and S. Wahlborn, Arkiv Fysik 16, 545 (1960).

[12] S. A. Moszkowski, in *Alpha-, Beta-, and Gamma-ray Spectroscopy*, edited by K. Siegbahn (North-Holland Publishing Company, Amsterdam, The Netherlands, 1965), Vol. 2, p. 863.

[13] H. Ejiri and J. P. Bondorf, Phys. Letters 28B, 304 (1968).